

Increasing linear flux range of SQUID amplifier using self-feedback effect

Ying-Yu Chen(陈滢宇), Chao-Qun Wang(王超群), Yuan-Xing Xu(徐元星), Yue Zhao(赵越), Li-Liang Ying(应利良), Hang-Xing Xie(谢颃星), Bo Gao(高波), and Zhen Wang(王镇)
Citation: Chin. Phys. B, 2023, 32 (**11**): 118501. DOI: 10.1088/1674-1056/acd8ac
Journal homepage: http://cpb.iphy.ac.cn; http://iopscience.iop.org/cpb

What follows is a list of articles you may be interested in

Multiplexing technology based on SQUID for readout of superconducting transition-edge sensor arrays

Xinyu Wu(吴歆宇), Qing Yu(余晴), Yongcheng He(何永成), Jianshe Liu(刘建设), and Wei Chen(陈炜)
Chin. Phys. B, 2022, 31 (**10**): 108501. DOI: 10.1088/1674-1056/ac693c

Development of series SQUID array with on-chip filter for TES detector

Wentao Wu(伍文涛), Zhirong Lin(林志荣), Zhi Ni(倪志), Peizhan Li(李佩展), Tiantian Liang(梁恬恬), Guofeng Zhang(张国峰), Yongliang Wang(王永良), Liliang Ying(应利良), Wei Peng(彭炜), Wen Zhang(张文), Shengcai Shi(史生才), Lixing You(尤立星), and Zhen Wang(王镇)
Chin. Phys. B, 2022, 31 (**2**): 028504. DOI: 10.1088/1674-1056/ac2b91

Micro-scale photon source in a hybrid cQED system

Ming-Bo Chen(陈明博), Bao-Chuan Wang(王保传), Si-Si Gu(顾思思), Ting Lin(林霆), Hai-Ou Li(李海欧), Gang Cao(曹刚), and Guo-Ping Guo(郭国平)
Chin. Phys. B, 2021, 30 (**4**): 048507. DOI: 10.1088/1674-1056/abe29b

Controllable microwave frequency comb generation in a tunable superconducting coplanar-waveguide resonator

Shuai-Peng Wang(王帅鹏), Zhen Chen(陈臻), and Tiefu Li(李铁夫)
Chin. Phys. B, 2021, 30 (**4**): 048501. DOI: 10.1088/1674-1056/abc2bb

Characterization of barrier-tunable radio-frequency-SQUID for Maxwell's demon experiment

Gang Li(李刚), Suman Dhamala, Hao Li(李浩), Jian-She Liu(刘建设), Wei Chen(陈炜)
Chin. Phys. B, 2018, 27 (**6**): 068501. DOI: 10.1088/1674-1056/27/6/068501

Increasing linear flux range of SQUID amplifier using self-feedback effect

Ying-Yu Chen(陈滢宇)[1,3,4], Chao-Qun Wang(王超群)[1,3,4], Yuan-Xing Xu(徐元星)[2], Yue Zhao(赵越)[1,3,4], Li-Liang Ying(应利良)[1,3,4], Hang-Xing Xie(谢颃星)[2], Bo Gao(高波)[1,3,4,†], and Zhen Wang(王镇)[1,3,4]

[1] *Shanghai Institute of Microsystem and Information Technology, Chinese Academy of Sciences (CAS), Shanghai* 200050, *China*
[2] *Shanghai Institute of Optics and Fine Mechanics, Chinese Academy of Sciences, Shanghai* 201800, *China*
[3] *CAS Center for Excellence in Superconducting Electronics (CENSE), Shanghai* 200050, *China*
[4] *University of Chinese Academy of Sciences, Beijing* 100049, *China*

(Received 15 February 2023; revised manuscript received 15 May 2023; accepted manuscript online 25 May 2023)

Superconducting quantum interference devices (SQUIDs) are low-noise amplifiers that are essential for the readouts of translation edge sensors (TESs). The linear flux range is an important parameter for SQUID amplifiers, especially those controlled by high-bandwidth digital flux-locked-loop circuits. A large linear flux range conduces to accurately measuring the input signal and also increasing the multiplexing factor in the time-division multiplexed (TDM) readout scheme of the TES array. In this work, we report that the linear flux range of an SQUID can be improved by using self-feedback effect. When the SQUID loop is designed to be asymmetric, a voltage-biased SQUID shows an asymmetric current–flux (I–Φ) response curve. The linear flux range is improved along the I–Φ curve with a shallow slope. The experimental results accord well with the numerical simulations. The asymmetric SQUID will be able to serve as a building block in the development of the TDM readout systems for large TES arrays.

Keywords: translation edge sensors, superconducting quantum interference device (SQUID), self-feedback

PACS: 85.25.Dq, 85.25.Oj **DOI:** 10.1088/1674-1056/acd8ac

1. Introduction

Transition edge sensors (TESs) are high-performance energy-resolved photon detectors, which are the key components of the Hot Universe Baryon Surveyor (HUBS), a proposed Chinese space x-ray telescope aiming to search for the so-called "mission baryons".[1] The detector array of HUBS consists of more than 3600 TES pixels. To read such a large number of low temperature detectors, a multiplexed readout technique is required to reduce the number of cables that connect superconducting quantum interference device (SQUID) amplifiers with room temperature electronics.[2] Otherwise, the thermal loads caused by the cables may exceed the cooling power of the cryo-cooler. A multiplexed readout is also indispensable for a space mission to meet the critical requirements for the weight and power consumption of the readout electronic system. Time-division multiplexing (TDM) is a mature multiplexed readout technique,[3] and it is considered as a candidate readout technique for HUBS. The basic idea of TDM is to connect a certain number of sensor SQUID amplifiers in series and each individual sensor SQUID is coupled with one TES pixel. The signal from each individual TES pixel can be amplified sequentially by activating the sensor SQUIDs one by one, and the multiplexed readout is realized. The number of TES pixels in one readout module is the multiplexing (Mux) factor of the TDM system.[4] The larger this number, the less readout modules are needed. The Mux factor N is constrained by the maximal tolerable readout noise and also by the linear flux range of the sensor SQUID amplifier. The TDM technique suffers a noise penalty because of the enhanced noise bandwidth, which is scaled up linearly with the Mux factor. Therefore, the current noise of the TDM readout is scaled up with $N^{1/2}$. The TDM usually incorporates a digital flux-locked loop (DFLL) technique.[5] All the sensor SQUIDs in a readout module are initially locked to their own working points. During operation, the error signal (the deviation from the initial locking point) of each sensor SQUID is measured. The error signal is used to calculate the flux feedback signal,which will be used in the next time frame to restore the sensor SQUIDs back to their working points. Proper working of the DFLL circuit should keep the error signal within the linear flux range of the sensor SQUID.[6] The flux variation between two successive readouts of one sensor SQUID needs to be less than its linear flux range, and satisfy the following condition:

$$\Delta\Phi = M_{\rm in}\cdot N\cdot t_{\rm row}\cdot\left|\frac{{\rm d}I}{{\rm d}t}\right|{\rm max} < c\cdot{\rm LFR}\cdot\Phi_0, \tag{1}$$

where $M_{\rm in}$ is the mutual inductance of the input coil of the sensor SQUID, $t_{\rm row}$ is the dwell time for each sensor SQUID in one-time frame, N is the Mux factor, ${\rm d}I/{\rm d}t({\rm max})$ is the maximal slew rate of the current signal generated by the TES, LFR

†Corresponding author. E-mail: bo_f_gao@mail.sim.ac.cn
© 2023 Chinese Physical Society and IOP Publishing Ltd

is the linear flux range normalized to one flux quantum, and c is a factor referring to the percentage of the linear flux range allocated to the rising edge of the TES current signal.[7] Increasing the flux range raises the upper limit of the Mux factor N and makes a higher mutual inductance feasible, which also conduces to reducing the current noise of the SQUID amplifier. In this paper, we present a method to increase the linear flux range by designing a sensor SQUID with asymmetric loop inductance. Both numerical simulations and the experimental characterizations are conducted.

2. Design of asymmetric SQUID

2.1. Self-feedback effect

A DC SQUID consists of two Josephson junctions embedded in a superconducting loop. The superconducting loop is usually divided into two branches, as schematically shown in Figs. 1(a) and 1(b). The inductances of the two branches, denoted as $L_{\rm left}$ and $L_{\rm right}$, can be equal or different, depending on where the bias current flows into/out of the superconducting loop. The critical current of the SQUID is tuned by the magnetic flux through the superconducting loop. The total magnetic flux through the SQUID is the sum of the externally applied flux and the flux generated by the current that flows through the SQUID. If the inductance of the left branch and the right branch are equal, the bias current flows symmetrically through both branches and the net magnetic flux produced by the bias current is zero. If the inductances $L_{\rm left}$ and $L_{\rm right}$ are not equal, the current in the left branch and the right branches will be different. Therefore, the bias current of the SQUID will contribute to the total magnetic flux through the SQUID.[8] Inspired by the talk of Irwin,[9] we call this the self-feedback effect, and we study its influence on the SQUID response to an externally applied flux.

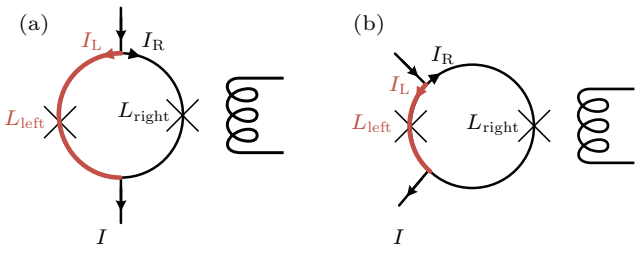


Fig. 1. Schematic diagram of (a) symmetric and (b) asymmetric SQUID loop design.

2.2. Numerical simulations of SQUID responses

We numerically simulate the response of SQUID to an externally applied flux for the SQUID designs as shown in Figs. 1(a) and 1(b). The simulation is a transient analysis in the time domain, and the externally applied flux is realized by a piecewise linear sweep current. Table 1 gives the simulation parameters of both SQUIDs. The parameters are derived from the geometry of the SQUID designs and from the known fabrication process parameters. We simulate the response of current-biased SQUID and voltage-biased SQUID to the externally applied flux. In the voltage-biased case, a bias resistor with a resistance of 0.5 Ω is connected in parallel with the SQUID.[10] We simulate the currents flowing through the left branch and the right branch of the SQUID loop, which vary with externally applied flux.

Table 1. Simulation parameters.

Variable	Parameter	Symmetric SQUID	Asymmetric SQUID
$I_{\rm c}$ (μA)	critical current	7.8	7.8
$C_{\rm jj}$ (fF)	JJ capacitance	315.8	315.8
$R_{\rm s}$ (Ω)	shunt resistance	7.6	7.6
$M_{\rm left}$ (pH)	mutual inductance	89.9	89.9
$M_{\rm right}$ (pH)	mutual inductance	89.8	89.8
$L_{\rm left}$ (pH)	left branch inductance	68.5	119.7
$L_{\rm right}$ (pH)	right branch inductance	68.5	17.3

Figures 2(a) and 2(b) show the results for current-biased SQUIDs. The bias current is set to 16.2 μA, which is slightly greater than $2I_{\rm c}$. For the two SQUID designs, the currents flowing through the left branch ($I_{\rm left}$) and the right branch ($I_{\rm right}$) are mirror images of each other, so the total current through the SQUID is a constant. In both cases, the V–Φ curve does not show any asymmetry, and the slopes along the positive and negative sides are equal to each other. The difference in the SQUID design only results in a phase shift in the V–Φ curve. For the symmetric design, the maximum of the V–Φ curve appears at $\Phi/2$, whereas for the asymmetric design, the maximum deviates from that position.

Figures 2(c) and 2(d) show the results for the voltage-biased SQUIDs. The bias current is set to 20.9 μA. Figure 2(c) shows the simulation results for a symmetrically designed SQUID. The branch currents $I_{\rm left}$ and $I_{\rm right}$ are expected to be identical, which is confirmed by the simulation. The slight phase shift is caused by the time delay when the flux bias current flows through two series-connected input inductors, one of which is coupled to $L_{\rm left}$ and the other is coupled to $L_{\rm right}$. The total current through the SQUID, which is the sum of $I_{\rm left}$ and $I_{\rm right}$, is also shown by the black dotted line. As seen in the figure, the $I_{\rm total}$–Φ curve is symmetric.

We now turn to the SQUID with asymmetric loop inductance. As seen in Fig. 2(d), the current flowing through the left branch and the current flowing through the right branch are significantly different from each other. The modulation depth is higher for the current flowing through the branch with lower inductance. The $I_{\rm total}$–Φ curve is asymmetric with the positive slope steeper than the negative slope.

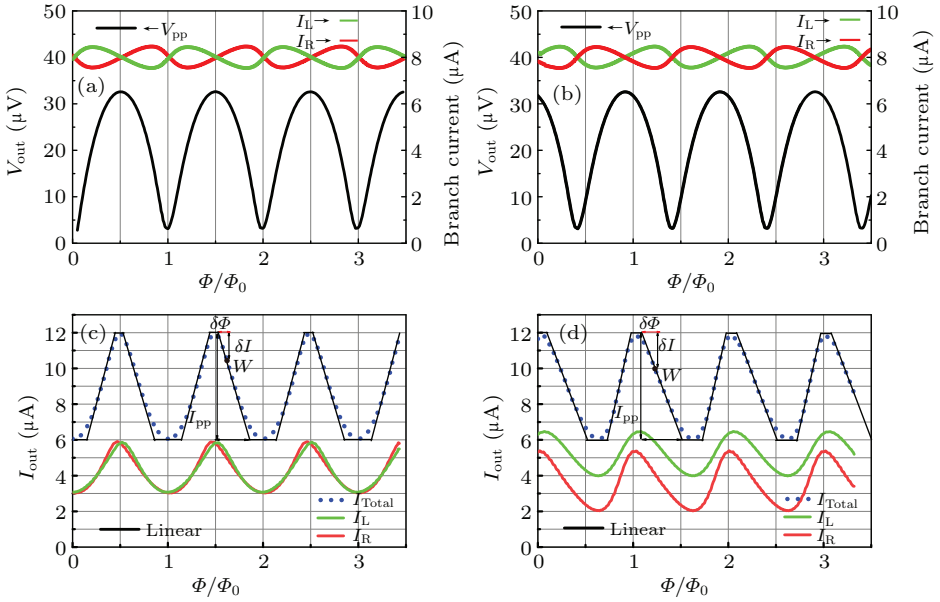


Fig. 2. The V–Φ curves of (a) symmetric and (b) asymmetric SQUID under current bias. Simulated I–Φ curves of (c) symmetric and (d) asymmetric SQUID under voltage bias, with black straight lines representing linear fits.

We compare the values of linear flux range $\Phi_{\rm lin}$ of the SQUIDs under voltage bias. The linear flux range depends on the working-point of the SQUID. We usually set the working point on the I–Φ curve where the slope is maximized to obtain an optimal noise performance. In Figs. 2(c) and 2(d), the I–Φ curves are approximated by the solid lines.[11] $2\delta I$ is the usable current swing range and the transfer coefficient at the working point is defined as $I_\Phi = \delta I/\delta\Phi$. The linear flux range is defined as $2\delta\Phi$. For the symmetric SQUID design, the transfer coefficient calculated at the chosen working point is 18 μA/Φ, and the corresponding linear flux range is 0.23Φ. For the asymmetric SQUID design, the transfer coefficient at the working point is 12 μA/Φ, and the linear flux range is 0.32Φ. The linear flux range is expanded by 45% in the latter case.

2.3. Experimental characterizations

We fabricate the SQUID devices described above by using the standard Nb–(Al–AlO_X)–Nb Josephson devices fabrication process developed at the Shanghai Institute of Microsystem and Information Technology.[12]

To measure the I–Φ curve of a voltage-biased sensor SQUID, we set up the circuit shown in Fig. 3. The sensor SQUID is inductively loaded with the input coil of an SQUID series array (SSA) amplifier. The SSA contains 16 single SQUIDs, and it operates in the flux-locked-loop (FLL) mode and acts as a current-to-voltage amplifier.[13] The trans-impedance gain of the SSA is

$$G_{\rm FLL} = \frac{\Delta V}{\Delta I_{\rm in}} = \frac{M_{\rm in}}{M_{\rm rb}} \cdot R_{\rm fb}. \tag{2}$$

We use a feedback resistor with a resistance of about 10 kΩ, and the input mutual inductance of the SSA, $M_{\rm in}$, is approximately equal to the feedback mutual inductance $M_{\rm rb}$. The trans-impedance gain of the SSA in the FLL mode is roughly 10 kΩ. A 200-Hz triangular wave signal is applied to the input coil of the sensor SQUID to visualize the I–Φ curve. The amplitude of the triangular wave signal is set to 40 μA. The bias resistance Rb is about 0.5 Ω and the bias current is set to 21 μA.

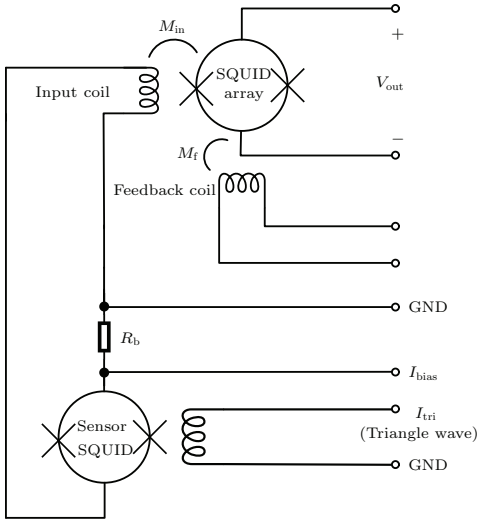


Fig. 3. Schematic diagram for measuring I–Φ curve of sensor SQUID.

Figures 4(a) and 4(b) show the simulated and measured I–Φ curves of the symmetric SQUID and asymmetric SQUID. The simulated curves match well with the experimental curves. Figures 4(c) and 4(d) each show the linear flux range deduced from the experimental curve. The transfer coefficient at the working point and the linear flux range for the symmetric SQUID design are 19 μA/Φ and 0.25Φ; while the corresponding values for the asymmetric SQUID design are 13 μA/Φ and 0.36 Φ. The experimental results confirm that the asymmetric SQUID design improves the linear flux range.

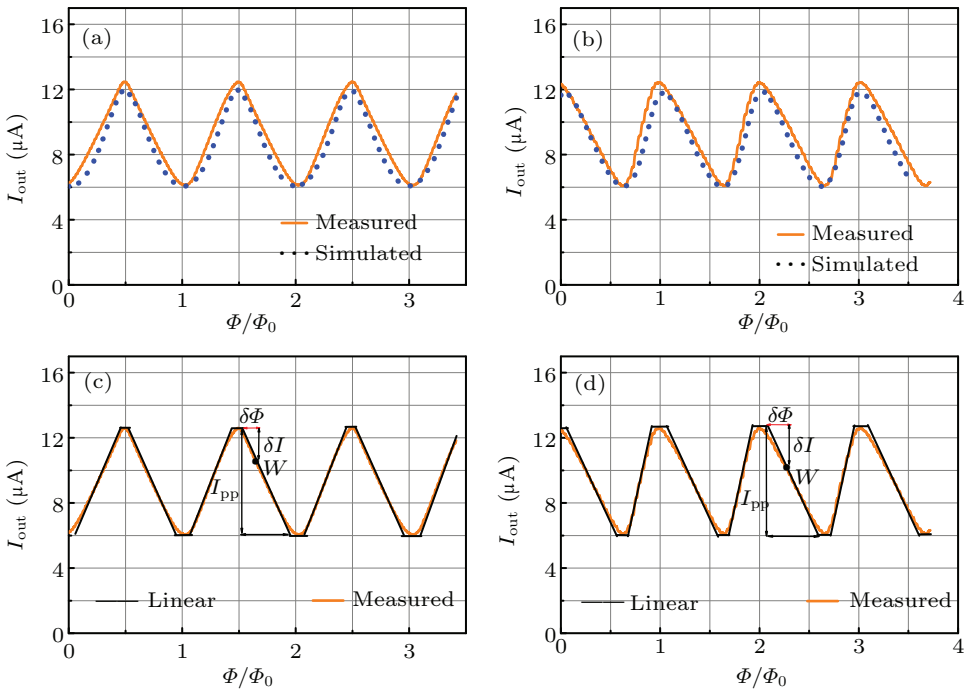


Fig. 4. Comparison of simulated and experimental I–Φ curves between (a) symmetric SQUID and (b) asymmetric SQUID. Measured linear flux ranges for (c) symmetric SQUID and (d) asymmetric SQUID, with solid lines representing experimental curves and black straight lines referring to linear fits.

3. Conclusions

We designed an asymmetric SQUID by putting most of the SQUID loop inductance on one side of the SQUID loop. The self-feedback effect leads to an asymmetric I–Φ curve of the voltage-biased SQUID, which can be seen in the numerical simulations and also confirmed by the experimental measurements. The linear flux range is enhanced along the negative slope side of the I–Φ curve. Sensor SQUIDs that adopt such a design can be used to develop a two-stage TDM readout system for TES array.

Acknowledgements

We thank Dr. Jie Ren for providing SFQ design infrastructure and Mark R. Kurban for drafting this manuscript.

Project supported by the Fund from China National Space Administration (CNSA) (Grant No. D050104) and the Fund for Low Energy Gamma Ray Detection Research Based on SQUID Technique, the Superconducting Electronics Facility (SELF) of Shanghai Institute of Microsystem and Information Technology, Chinese Academy of Sciences.

References

[1] Cui W, Bregman J N, Bruijn M P, *et al.* 2021 *Proc. SPIE* 11444
[2] Dobbs M A, Halpern M, Irwin K D, Lee A T, Mates J A B and Mazin B A 2009 *J. Phys. Conf. Ser.* **155** 012004
[3] Doriese W B, Morgan K M, Bennett D A, *et al.* 2016 *J. Low Temp. Phys.* **184** 389
[4] Chervenak J, Irwin K D, Grossman E, Martinis J, Reintsema C D and Martin H 1999 *Appl. Phys. Lett.* **74** 4043
[5] Reintsema C D, *et al.* 2009 *AIP Conf. Proc.* **1185** 237
[6] Smith S J, Adams J S, Bandler S R, *et al.* 2021 *IEEE Trans. Appl. Supercond.* **31** 2100806
[7] Durkin M, Adams J S, Bandler S R, *et al.* 2019 *IEEE Trans. Appl. Supercond.* **29** 2101005
[8] Mangin P and Kahn R 2017 *Superconductivity: an Introduction*, 3rd edn. (Switzerland: Springer) pp. 306–308
[9] Irwin K D and Huber M E 2001 *IEEE Trans. Appl. Supercond.* **11** 1265
[10] Polushkin V, Glowacka D, Hart R and Lumley J M 2000 *J. Low Temp. Phys.* **118** 105
[11] Drung D 1996 *SQUID Sensors: Fundamentals, Fabrication and Applications* (Dordrecht: Springer), pp. 63–116
[12] Ying L L, Zhang X, Niu M H, Ren J, Peng W, Maezawa M and Wang Z 2021 *IEEE Trans. Appl. Supercond.* **31** 1301504
[13] Drung D 2002 *Physica C* **368** 134